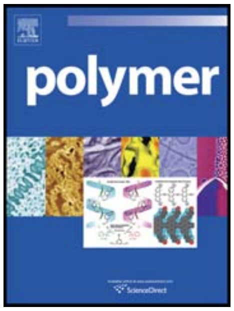

Well-Defined Second-Order Nonlinear Optical Polymers by Controlled Radical Polymerization, via Multifunctional Macromolecular Chain Transfer Agent: Design, Synthesis, and Characterizations

Anne-Lise Roy, Chong Bui, Ileana Rau, François Kajzar, Bernadette Charleux, Maud Save, David Kreher, André-Jean Attias

PII: S0032-3861(13)01177-4
DOI: 10.1016/j.polymer.2013.12.059
Reference: JPOL 16696

To appear in: *Polymer*

Received Date: 20 November 2013
Revised Date: 24 December 2013
Accepted Date: 27 December 2013

Please cite this article as: Roy A-L, Bui C, Rau I, Kajzar F, Charleux B, Save, M, Kreher D, Attias A-J, Well-Defined Second-Order Nonlinear Optical Polymers by Controlled Radical Polymerization, via Multifunctional Macromolecular Chain Transfer Agent: Design, Synthesis, and Characterizations, *Polymer* (2014), doi: 10.1016/j.polymer.2013.12.059.

Well-Defined Second-Order Nonlinear Optical Polymers by Controlled Radical Polymerization, via Multifunctional Macromolecular Chain Transfer Agent: Design, Synthesis, and Characterizations.

Anne-Lise Roy, Chong Bui, Ileana Rau, François Kajzar, Bernadette Charleux, Maud Save, David Kreher, André-Jean Attias*

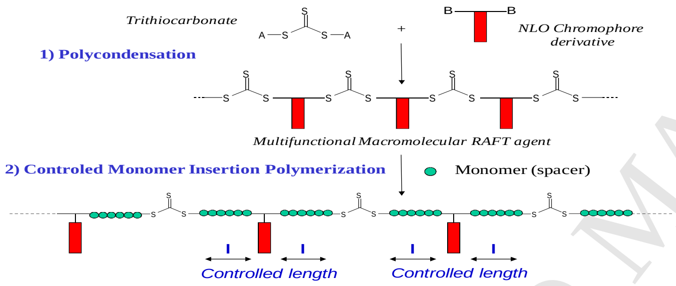

Well-Defined Second-Order Nonlinear Optical Polymers by Controlled Radical Polymerization, via Multifunctional Macromolecular Chain Transfer Agent: Design, Synthesis, and Characterizations.

Anne-Lise Roy,[1] Chong Bui,[1] Ileana Rau,[2] François Kajzar,[2,3] Bernadette Charleux,[4] Maud Save,[5] David Kreher, [1,6] André-Jean Attias[1]*

1 UMR 7610 CNRS – UPMC, Laboratoire de Chimie des Polymères, 3 rue Galilée, 94200 Ivry, France.

andre-jean.attias@upmc.fr.

2 University POLITEHNICA of Bucharest, Faculty of Applied Chemistry and Materials Science, Dept. of General Chemistry, 1 Polizu Street, 011061 Bucharest, Romania.

3 Institut des Sciences et Technologies Moléculaires d'Angers, MOLTECH Anjou – UMR CNRS 6200, Université d'Angers, 2 bd Lavoisier, 49045 Angers Cedex, France.

4 Université de Lyon, Univ. Lyon 1, CPE Lyon, CNRS, UMR 5265, Laboratoire de Chimie, Catalyse, Polymères et Procédés (C2P2), LCPP group, 43, Bd. du 11 Novembre 1918, F-69616 Villeurbanne, France.

5 CNRS, University of Pau & Pays Adour, UMR 5254, IPREM, Equipe de Physique et Chimie des Polymères, 2 avenue du Président Angot, Pau, F-64053, France

6 ENSTA – Synthèse Organique et Réactivité, Ecole Polytechnique – UMR CNRS 7652, 91128 Palaiseau Cedex, France.

† Electronic supplementary information (ESI) available: The NLO set-up description is given, this material being available free of charge.

Abstract

To address the issue of the aggregation in second-order nonlinear optical (NLO) polymers we developed an approach based on the synthesis of a multifunctional macromolecular chain transfer agent. The controlled monomer insertion polymerization into the main chain by a ‘reversible addition-fragmentation chain transfer’ (RAFT) mechanism allows the spatial arrangement of the NLO chromophores along the polymeric chain in order to obtain sequence-ordered polymers. In a first step, a novel trithiocarbonate based macroinitiator containing the disperse red 19 (DR19) units in the main chain was synthesized by polycondensation; in a second step, this polymeric precursor was applied to the synthesis of a sequentially ordered polymer by controlled insertion radical polymerization of styrene. Size exclusion chromatography (SEC), nuclear magnetic resonance (NMR) data revealed that, (i) for the first time, polystyrenes (PS) bearing DR19 dyes covalently bounded were obtained, and (ii) both the insertion reaction and the length of the polystyrene segments were accurately controlled. Whatever the incorporated dye amount, all the copolymers were soluble in common solvents. Second-order optical nonlinearity in corona-poled thin films was evaluated, and second harmonic coefficients up to 80 pm/V were determined for loading ratio lower than 10 wt-% (DR19/PS). This approach opens up opportunities for the incorporation of more efficient chromophores even in apolar matrices.

Introduction

Organic second-order nonlinear optical (NLO) polymers have attracted considerable attention in the past two decades for their potential applications in information processing and telecommunications [1-2]. The interest in these materials derives from the high electro-optic (E-O) coefficients (r_{33}) measured with NLO chromophore-containing polymeric materials [3-4]. In general, an E-O polymer system consists of NLO chromophores dispersed in a host matrix (guest-host system) or covalently attached to a polymer backbone (side-chain polymer, main chain polymer), the second-order nonlinear effect resulting from an asymmetric alignment of the chromophores using electric field poling.

Currently, one of the most challenging task in the 2^{nd} order NLO polymeric material development is to efficiently translate molecular optical nonlinearity (β) into macroscopic second-order NLO activity (second harmonic generation, electro-optic modulation, optical rectification etc, that is to say to reduce chromophore-chromophore interactions in the bulk state) [5-6]. First, a majority of the efforts addressing the improvement of the E-O polymer performances have concentrated on the systematic design of chromophores with large hyperpolarizability (β) [7]; second, beside increasing the number and efficiency of chromophores, efforts were mainly devoted to improve poling efficiency.

In this purpose, several strategies have been proposed, such as either optimization of the guest-host interactions in the case of doped polymers [8-9], or matrix/chromophore compatibility improvement, or self-assembly, and/or shape engineering of the chromophores [10-13]. The latter approach has been intensively studied through the nanoscale tailoring of NLO chromophores and polymers leading to dendritic modified NLO chromophores [10, 14-17], side-chain dendronized NLO polymers [18-19], pendant diazobenzene NLO linear polymers [20-21] or crosslinkable polymers via Diels-Alder type reaction for lattice hardening [22-26]. In the latter case, the poled/cured polymers showed very large E-O coefficients (up to 263 pm/V at the wavelength of 1.31 µm).

Here, we propose an alternative complementary way to minimize the chromophore-chromophore interactions, based on controlled radical polymerization. To validate this approach, we will use a non polar matrix (polystyrene, PS) which usually leads to poor solvatation of highly polar chromophores, resulting in very low electro-optic (E-O) coefficients (r_{33}) (0.5 for 10% wt chromophore ratio) [8]. This strategy enables us to expect the synthesis of polystyrene containing NLO chromophore groups distributed homogeneously along the polymer chain and separated by PS blocks with narrow dispersity.

Since their emergence in the nineties, the controlled radical polymerization (CRP) methods [27], recently named by IUPAC reversible deactivation radical polymerization (RDRP) [28], have known an increasing interest as they proved to be efficient methods to control the macromolecular architectures (molar masses, narrow chain length distribution and topology) while preserving the versatility and the easy implementation of radical polymerization. The design of various polymers with complex topologies has been possible by the development of different CRP techniques: nitroxide-mediated living free-radical polymerization (NMP) [29-30], atom transfer radical polymerization (ATRP) [27, 31-32], reversible addition fragmentation chain transfer (RAFT) [33-34], cobalt-mediated radical polymerization [35] and organotellurium-mediated living radical polymerization (TERP) [36]. Among these methods, RAFT and NMP allowed the synthesis of multisegmented polymers via the vinylic monomer insertion into either a multifunctional polyalkoxyamine macro-initiator [37-39], or a multifunctional macromolecular RAFT agent [40-48]. Well-defined multiblock copolymers were successfully prepared by this way [36-40, 46, 49]. Multisegmented polymers have also been prepared by consecutive radical addition-coupling reaction of α,ω-macrobiradicals onto nitroso compound [50], dithioester [51], dinitroxides [52] or by click chemistry of telechelic polymers synthesized by RAFT and ATRP polymerization [53-54]. A theoretical study highlighted that multiblock copolymers of higher homogeneity are rather prepared with RAFT strategy through a polyfunctional chain transfer agent than with the commonly used coupling of functionalized prepolymers [55]. The originality of the present study lies in the synthesis of a chromophore based polyfunctional RAFT agent to implement the synthesis of a multisegmented polymer with the block interconnected by the functional group.

Experimental section

Chemicals. All commercially available chemicals were used without further purification. Solvents were carefully dried and distilled prior to use. All glassware was also heat-dried under vacuum with a hot air gun before using. Reactions were performed under an inert atmosphere. Column chromatography was performed on Geduran Silica 60 (40-63 μm, Merck). Styrene (Acros, 99 %) was distilled under vacuum before use. Carbon disulfide (Acros, 99%), nonahydrated sodium sulphur (Extra pur, Acros), methyltributylammonium chloride (Aldrich, 75 wt-% in water), 2-bromopropionyl bromide (Aldrich, 96%), Disperse Red 19 (Aldrich, 96 %), triethylamine (Acros, 99 %), tetrabutylammonium hydrogensulfate (TBAHS, Aldrich, 97%), azo-bis-isobutyronitrile (AIBN, Fluka, 98 %) were used as supplied.

Monomer Synthesis. *Synthesis of Trithiocarbonate disodium in aqueous solution* ***(1)*****.** Carbon disulfide (6.6 g, 0.087 mol) was slowly added to a mixture of nonahydrated sodium sulfur (0.083

mol), methyltributylammonium chloride (0.42 g, 1.8 mmol) and water (28 mL). After stirring for one night at ambient temperature, a red aqueous solution was recovered and stored at 4 °C.

*Synthesis of DR19-di-2-bromopropionate **(2)***. 2-bromopropionyl bromide (13 mL, 0.121 mol) in anhydrous tetrahydrofuran (50 mL) was added dropwise under stirring to a cooled solution containing Disperse Red 19 (6.1 g, 0.018 mol) and triethylamine (17 mL, 0.121 mol) in 100 mL anhydrous tetrahydrofurane. The solution was stirred at room temperature for 48h. Additional water (100 mL) was added to dissolve the triethylamine bromohydrate salts. The organic phase was extracted with diethyl ether, washed with a saturated aqueous solution of $NaHCO_3$ (50 mL), and water (3 × 50 mL) until neutral pH of the aqueous phase was reached, dried over $MgSO_4$, filtered and solvent was evaporated. The crude product was purified by column chromatography on silica gel, using dichloromethane as an eluent, to give 7.5 g of a red solid (yield = 68 %).

^1H NMR (*$CDCl_3$*; 200 MHz) δ (ppm): 1.79 (d, 6H, ^3J = 7.0 Hz, C**H**$_3$), 3.83 (t, 4H, ^3J = 6.2 Hz, C**H**$_2$-N), 4.43 (m, 6H, C**H**-Br, C**H**$_2$-O), 6.87 (d, 2H, ^3J = 9.2 Hz, C**H**$_{arom}$), 7.93 (d, 2H, ^3J = 9.2 Hz, C**H**$_{arom}$), 7.95 (d, 2H, ^3J = 9.2 Hz, C**H**$_{arom}$), 8.35 (d, 2H, ^3J = 9.2 Hz, C**H**$_{arom}$).

Multifunctional Macromolecular RAFT Agent (MM-RAFT): synthesis of DR19-based polytrithiocarbonate (3). The DR19-di-2-bromopropionate and the crude aqueous solution of disodium trithiocarbonate were used for the synthesis of the desired DR19-based polytrithiocarbonate by step polymerization. DR19-di-2-bromopropionate (2.08 g, 3.5 mmol), tetrabutylammonium hydrogensulfate (240 mg, 0.7 mmol) as phase transfer catalyst, toluene (14 mL), and the solution of sodium trithiocarbonate in water (12 mL, 3.5 mmol) were introduced into a round-bottom flask. The mixture was stirred at 60 °C for 72 h. The organic phase was extracted with diethyl ether, washed with water (4 × 50 mL), dried over $MgSO_4$, filtered and solvent was evaporated. The crude product was purified by column chromatography (diameter = 15 cm; height = 1 m) on silica gel, using a 1:1, v:v, cyclohexane:dichloromethane mixture, then pure dichloromethane, then a 1:3, v:v, ethyl acetate:dichloromethane mixture as an eluent, to give several fractions, one consisting in 1.2 g of a red solid (yield = 47 %). The fraction of DR19-based polytrithiocarbonate recovered for subsequent RAFT polymerization of styrene displayed the following macromolecular characteristics: $M_{n,\ MM\text{-}RAFT} = 2690$ g.mol^{-1}, $M_w/M_n = 1.20$.

RAFT polymerization of styrene (4). A mixture of the prepared multifunctional macromolecular RAFT agent (515 mg, 1.92×10^{-4} mol, $M_n = 2685$ g.mol^{-1}, $M_w/M_n = 1.20$) and AIBN in solution in dichloromethane (3.84 mL, 5.19×10^{-5} mol) was stirred for 5 min. After evaporating the dichloromethane, distilled styrene (51.9 mL, 4.54×10^{-1} mol) was added. The mixture was stirred for 30 min and subsequently poured into six tubes sealed with Rotaflo®. Oxygen was removed by five freeze-vacuum-thaw cycles. The tubes were immersed into an oil bath thermostated at 70°C. Samples were withdrawn at regular time intervals (4 h, 8 h, 18 h and 48 h), quenched by cooling in water and exposed to air. After evaporating styrene under vacuum, the crude sample was weighed to determine the monomer conversion. The crude polymer was purified by dissolving into a minimum volume of dichloromethane prior to precipitation into cold methanol (below 0 °C). The purified polymer was subsequently dried under vacuum and characterized by SEC.

Techniques for chemical characterizations. *Nuclear Magnetic Resonance (NMR) Spectroscopy.* ^1H and ^{13}C NMR spectra were recorded on a Bruker ARX 250 instrument or a Bruker AC 200 instrument. Chloroform-*d* ($CDCl_3$) or dimethyl sulfoxyde-d_6 (DMSO-d_6) were used as the solvent. *Size Exclusion Chromatography (SEC).* The number-average molar mass

(M_n), the weight-average molar mass (M_w) and the molar mass distributions (polydispersity index = M_w/M_n) were determined by size exclusion chromatography using tetrahydrofuran (THF) as eluent at a flow rate of 1 mL·min^{-1}. The SEC apparatus was a Triple Detector Array (TDA, model 302 from Viscotek) equipped with both a refractive index detector and a viscosimeter (online measurement of the intrinsic viscosity $[\eta]$ by a Wheaston bridge) and three Polymer Laboratories Mixed C columns (5 µm) thermostated at 40°C. The average molar masses were derived from a universal calibration curve ($\mathrm{Log}([\eta].M) = f(\mathrm{Elution\ volume})$) based on polystyrene standards from Polymer Standards Service (separation limits: 260 – 2×10^6 g.mol^{-1}). The sample concentrations ranged from 7 to 10 mg/mL. The refractive index increment of the macromolecular RAFT agent was measured online (dn/dc = 0.23 L.g^{-1}). *Thermal analysis.* Melting points were measured on a TA Instruments DSC 2920-Modulated DSC operating at 5 °C/min under nitrogen. *UV-Visible spectroscopy.* UV-Visible spectrophotometric analysis of the polymers was performed in dichloromethane solution using a BIO-TEK Instruments UVIKON 923 spectrophotometer.

Film Preparation. Electrical Poling, and NLO Measurements. The studied thin films were obtained from polymer solutions by the spinning technique. Polymers were dissolved in 1-1-2 trichloroethane and spread on the carefully cleaned glass substrates. The typically used angular rotation speeds were 2000 tours/min, for both spreading and drying processes. After deposition the films were additionally dried in an oven at 80°C for about 2 hrs in order to remove the remaining solvent. The typical film thicknesses, measured with α tallystep, depending on polymer concentration and spinning speed, ranged between 100 and 200 nm. Chromophores were oriented by the corona poling technique and the SHG measurements were performed using a set-up described in supporting information.

Results and Discussion

In the present work, we propose the synthesis of a new multifunctional macromolecular RAFT agent containing NLO chromophores (DR19) incorporated along the chain via polyaddition [56] involving sodium trithiocarbonate and the dibromo derivative of the NLO chromophore (see **Scheme 1**, product **3**). The controlled insertion of polystyrene blocks into the DR19-based multifunctional macromolecular RAFT agent was carried out by controlled radical polymerization of styrene (**Scheme 1**, step **4**). The polar orientation of chromophores was obtained by the corona poling technique and the second order NLO properties were measured by the optical SHG. This technique measures the fast, electronic origin second-order NLO susceptibility tensor pp and sp components ($\chi^{(2)}_{pp}(-2\omega;\omega,\omega)=2d_{pp}$, $\chi^{(2)}_{sp}(-2\omega;\omega,\omega)=2d_{sp}$) where ω is the fundamental beam frequency. It allows to determine also the electronic parts of other second-order NLO susceptibilities of the studied material, including the electro-optic coefficient r.

In the present case the RAFT methodology was judiciously chosen for two reasons: a simple modification (*i.e*. esterification) of the NLO chromophore was required for its incorporation into the multifunctional macro-molecular RAFT agent and the RAFT mechanism can be implemented under mild polymerization temperature (70°C) avoiding the chromophore degradation.

For that purpose, an aqueous solution of trithiocarbonate disodium **1** was first obtained according to literature [57]. The chromophore DR19 was treated with 2-bromopropionyl bromide to afford the purified dibromo-compound 2 with a yield of 68%. The multifunctional macromolecular RAFT Agent **3** (MM-RAFT) containing DR19 units in the main chain was prepared by polycondensation of the dibromo-DR19 **2** with trithiocarbonate disodium 1 in the presence of TBAHS as a phase transfer catalyst (**Scheme 1**).

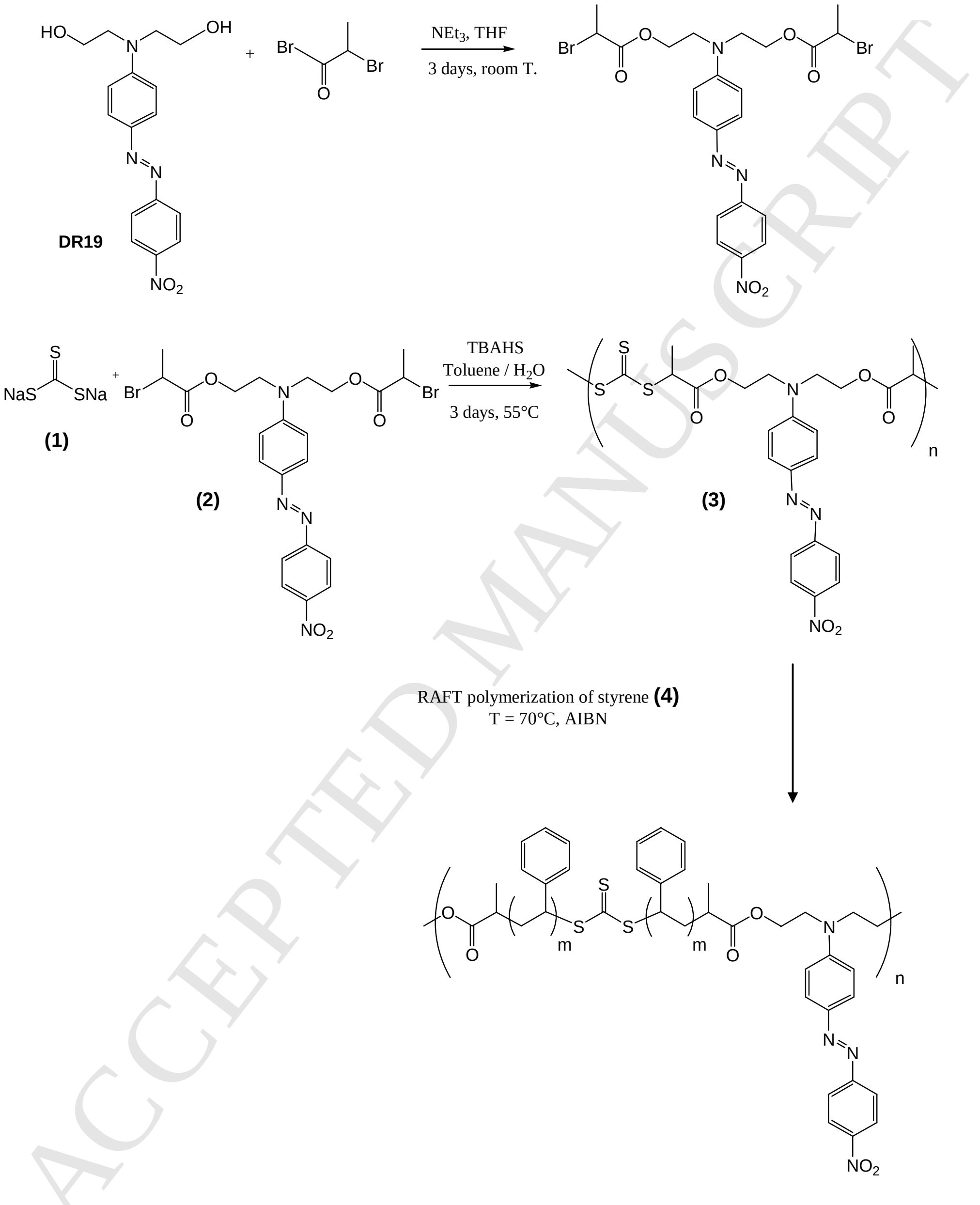

Scheme 1. General synthetic scheme for the synthesis of NLO polystyrene by controlled radical polymerization of styrene (**4**) via a DR19-based multifunctional macromolecular RAFT agent (**3**).

The polycondensation proceeded after mixing the monomers at 55°C for 3 days. The crude product was then purified by column chromatography to afford a low-dispersity DR19-based polytrithiocarbonate. The macromolecular characteristics of the resulting polymer **3** were estimated by size exclusion chromatography (SEC) using universal calibration. A fraction with a dispersity of 1.20 and number-average molar mass of 2690 g.mol^{-1} was used as macromolecular RAFT agent for the controlled insertion of styrene via controlled radical polymerization. Styrene was then polymerized at 70°C in bulk with **3** as a multifunctional macromolecular RAFT agent (**Scheme 1, Table 1**) and 2,2‘-Azobis(2-methylpropionitrile) (AIBN) as initiator.

Table 1. Bulk Polymerization of Styrene mediated by RAFT Polymerization Using the DR 19-based Polytrithiocarbonate as Multifunctional Macromolecular Transfer Agent (MM-RAFT): characteristics of the recovered polymers containing the DR19 dye.

Sample	1	2	3	4	5
Time (h)	0	4	8	18	48
Conversion (%)	0	2.6	5.9	13.5	16.4
M_n (theoretical) [b] (g.mol^{-1})	-	8000	15080	31030	37040
M_n (SEC) (g.mol^{-1})	2690	3820	12340	21550	27370
M_w/M_n	1.20	1.85	1.29	1.35	1.42
Wt-%$_{DR19}$ [c]	-	14.0	7.0	5.0	2.3
N_{DR19}		1.6	2.6	2.0	1.9

[a] Experimental conditions: [Styrene] = 8.7 mol.L^{-1}; [AIBN]$_0$ = 1 × 10^{-3} mol.L-1; [MM-RAFT] = 3.7 × 10^{-3} mol.L^{-1}; T = 70°C. [b] The theoretical molar mass of the styrene-based polymer was calculated as follows:

$$M_{n,theoretical} = M_{n,MM-RAFT} + \frac{[Styrene]_0}{[MM-RAFT]_0 + 0.6\times[AIBN]_0\times(1-e^{-k_d t})}\times conversion$$

with k_d the dissociation rate constant of the initiator ($k_{d,AIBN,70°C}$ = 4.72 × 10^{-5} s^{-1}) [58], the factor 0.6 corresponds to the AIBN efficiency for bulk polymerization (reference [59]) and the factor indicating the termination mechanism was considered equal to 1 as termination proceeds exclusively by combination for styrene polymerization. [c] Wt-%DR19 and N_{DR19} are respectively the weight percent of DR19 dye versus copolymer mass and the average number of DR19 per copolymer chain. The molar concentration of DR19 was calculated from the UV-visible absorbance (Abs) of the copolymer solution measured in methylene chloride inside a cell of 1 cm^2 using the Beer-Lambert law with ε_{DR19} = 36 000 mol.L^{-1}cm^{-1} at

472 nm. The weight percent of DR19 in the polymer was calculated as follows: $\mathrm{Wt-\%_{DR19}} = \frac{100\times[\mathrm{DR19}]_{\mathrm{mol}}\times \mathrm{M_{DR19}}}{[\mathrm{Copolymer}]_{\mathrm{wt}}}$ with M_{DR19} = 330 g.mol^{-1} and $[\mathrm{Polymer}]_{wt}$ = 0.1 g.L^{-1}.

The low polymerization rate of styrene polymerization carried out at 70 °C in the presence of the multifunctional RAFT agent was probably due to retardation phenomenon has already observed in some cases with trithiocarbonate RAFT agents [60].

The polymerization of styrene was controlled as highlighted by the linear evolution of molar masses (M_n) versus conversion (**Figure 1**) together with dispersity below 1.5. The higher value of dispersity at low conversion is characteristic of CRP mechanism [61] and this phenomenon is probably emphasized by the use of a relatively polydisperse multifunctional macromolecular transfer agent.

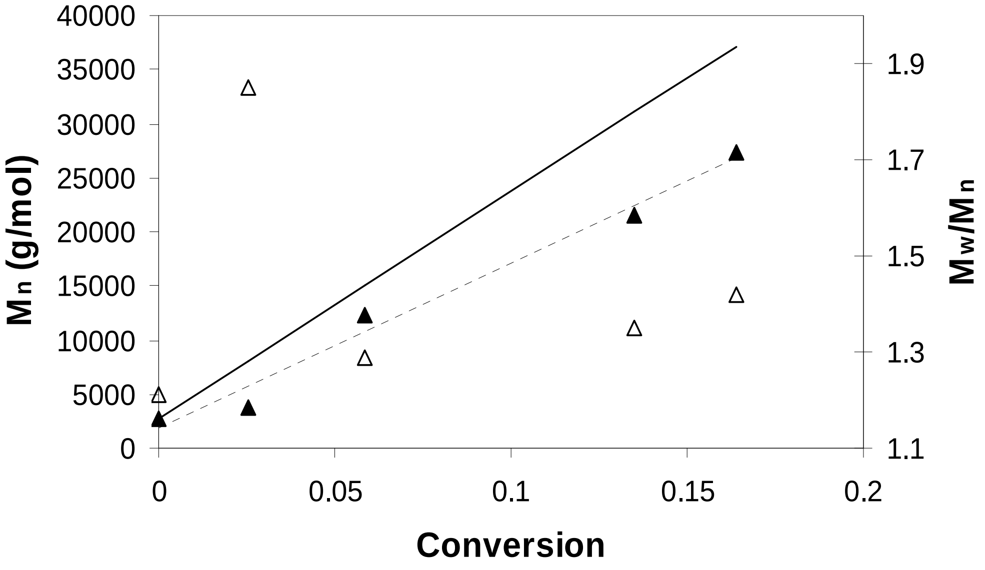

Figure 1. Evolution of M_n (plain) and $M_{w/}M_n$ (empty) versus conversion for the polymerization of styrene mediated by the DR19-based polytrithiocarbonate as "multifunctional macromolecular" RAFT agent. $[\mathrm{AIBN}]_0 = 1 \times 10^{-3}$ mol.L^{-1}; [MM-RAFT] = 3.7×10^{-3} mol.L^{-1}; T = 70°C. The plain line corresponds to the theoretical M_n.

The experimental M_n determined by a universal calibration were always below the theoretical M_n as displayed in **Figure 1**. The number of chains created by the initiator was considered for the calculation of the theoretical M_n (see Table 1), so the negative deviation indicates that other source than initiator is able to produce polymer chains. Thermal initiation of styrene polymerization for such long polymerization time can be a source of additional radicals.

These results showed that well-defined polystyrene blocks were inserted into the “multifunctional macromolecular” RAFT agent, hence suggesting a homogeneous distribution of the DR19 units along the polymer backbone. The polymers were analyzed by UV-visible absorption spectroscopy and we observed a maximum wavelength (λ_{max}) at 455 nm in dichloromethane, which corresponds to the λmax of DR19. The weight fraction of DR19 in the functional polymer could then be determined from the measured absorbance of these solutions at 455 nm (**Table 1**). The DR19 weight fraction logically decreased with the increase of styrene conversion, corresponding to the increase of styrene content through the controlled growth of PS blocks within the polymer.

Linear and non linear optical properties have been measured on thin films spin-coated from 1,1,2-trichloroethane (100 $g.L^{-1}$). Regarding linear optical properties, UV-visible absorption spectra (**Figure 2**) revealed that the films had a maximum absorption wavelength λmax of 458 nm. Extinction coefficients and the real parts of ordinary (n_o) and extraordinary (n_e) thin film refractive indices for the three studied concentrations are also displayed in **Figure 2**.

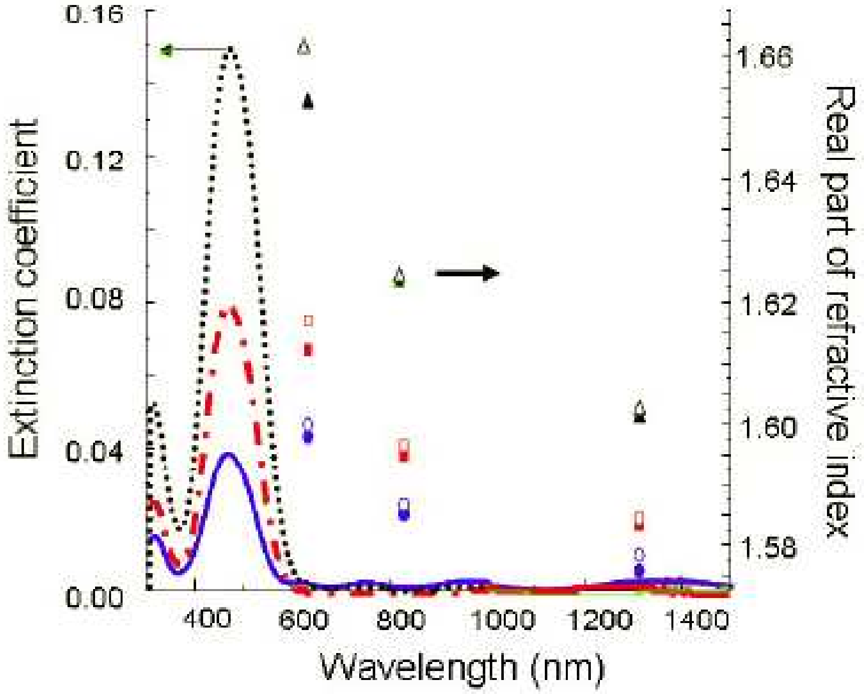

Figure 2. Wavelength dependence of the extinction coefficients *k* (solid lines, LHS) and indices of refraction (RHS) for studied thin films. Closed figures show ordinary (n_o) and open extraordinary (n_e) index of refraction, respectively. The highest curve and triangles correspond to the most concentrated films (7.0 wt %) whereas the lowest and diamonds to the less concentrated (2.3 wt %).

First, increasing the chromophore concentration leads to higher extinction coefficients values, as expected. Moreover, the observed Fabry-Perrot interference patterns behind the optical absorption spectra (λ > 600 nm) are fingerprints of a good thin film thickness homogeneity and low roughness (see supporting information).

The NLO properties of thin films were evaluated as follows. The films were poled by corona poling at 110 °C. Their second-order NLO susceptibilities, *dsp* and *dpp*, measured by the optical second harmonic generation are reported in **Table 2** for the two series of films at different chromophore concentrations.

For weight concentrations of DR19 lower than 7 %, the second harmonic generation (SHG) coefficients (*dsp* and *dpp*) increase linearly with the chromophore concentration (see also Figure SI-3 in Supporting Information). This observation is in favor of the absence (or limited) of aggregation in synthesized functional polymers [5, 62]. More precisely, very few studies previously reported the introduction of chromophores parent to DR19 into a polystyrene matrix in this range of DR19 weight concentrations. For instance, the Disperse red 1 (DR1) chromophore embedded into a polystyrene matrix led to a low d_{pp} value of 0.85 pm.V^{-1} characteristic of an aggregation phenomenon (see Supporting Information).[8]

Table 2: Second -order NLO susceptibilities *dsp* and *dpp* values of two thin polymer films (1 and 2) containing the DR19 chromophore at different weight fractions. The precision in *d* coefficient is ±10%.

Wt- % DR19	**2.3**	**5.0**	**7.0**
dsp 1 (pm.V^{-1})	12.9	14.9	28.6
dpp 1 (pm.V^{-1})	34.6	58.6	76.8
$a_1 = dpp_1/dsp_1$	2.7	3.9	2.7
dsp 2 (pm.V^{-1})	7.8	13.7	17.7
$a_2 = dpp_2/dsp_2$	3.7	3.6	4.2
dpp 2 (pm.V^{-1})	28.8	49.5	74.7

In **Table 2** we also listed the values of the ratio of two tensor components: $a = dpp\ /\ dsp$. Within the experimental accuracy, the values are close to 3, as usually observed in poled polymers. This result is a finger print of a moderate poling and agrees well with value predicted from gaz model of non-interacting chromophores.

Conclusions

In summary, we demonstrated that our chosen strategy based on controlled radical polymerization via a macromolecular multifunctional RAFT agent allows the synthesis of well-defined NLO polymers. More precisely, NLO chromophores are homogeneously distributed along the polymer backbone. Moreover, in spite of the non polar character of the polystyrene matrix, quite high *dsp* and *dpp* values have been obtained, without any aggregation evidence. These values are similar to the ones observed with poly(methyl methacrylate) (PMMA) matrix showing a similar DR19 chromophore loading amount (~ 10 wt-%). To conclude, the present synthetic strategy allows the controlled NLO chromophores insertion along the polymer backbone and solves the problem of aggregation in non polar matrices. Because of the versatility of the strategy, we offer a promising route to incorporate more efficient chromophores in a well-defined manner in other matrices such as PMMA for instance. More generally, this approach can be used in other fields where avoiding aggregation remains a key issue.

Acknowledgments

Authors F. K. and I. R. acknowledge the support of European Social Fund through the Sectorial Operation Programme Increasing Economical Competitivity, under POS CCE nr. 634, SMIS 12575. This work was supported by the French National Agency (ANR), within LUVORGAN project.

References

[1] Nalwa HS, Watanabe T, Miyata S. Nonlinear Optics of Organic Molecules and Polymers: CRC Press: Boca Raton, 1997.
[2] Prasad PN, Williams DJ. Introduction to Nonlinear Optical Effects in Molecules and Polymers. John Wiley & Sons: New York, 1991.

[3] Kajzar F, Lee KS, Jen AKY. Polymeric materials and their orientation techniques for second-order nonlinear optics. In: Lee KS, editor. Polymers for Photonics Applications Ii: Nonlinear Optical, Photorefractive and Two-Photon Absorption Polymers, vol. 161, 2003. pp. 1-85.

[4] Shi YQ, Zhang C, Zhang H, Bechtel JH, Dalton LR, Robinson BH, Steier WH. Science 2000;288(5463):119-122.

[5] Robinson BH, Dalton LR. Journal of Physical Chemistry A 2000;104(20):4785-4795.

[6] Robinson BH, Dalton LR, Harper AW, Ren A, Wang F, Zhang C, Todorova G, Lee M, Aniszfeld R, Garner S, Chen A, Steier WH, Houbrecht S, Persoons A, Ledoux I, Zyss J, Jen AKY. Chemical Physics 1999;245(1-3):35-50.

[7] Marder SR, Kippelen B, Jen AKY, Peyghambarian N. Nature 1997;388(6645):845-851.

[8] Banach MJ, Alexander MD, Caracci S, Vaia RA. Chemistry of Materials 1999;11(9):2554-2561.

[9] Priimagi A, Cattaneo S, Ras RHA, Valkama S, Ikkala O, Kauranen M. Chemistry of Materials 2005;17(23):5798-5802.

[10] Ma H, Chen BQ, Sassa T, Dalton LR, Jen AKY. Journal of the American Chemical Society 2001;123(5):986-987.

[11] Shi ZW, Liang W, Luo JD, Huang S, Polishak BM, Li XS, Younkin TR, Block BA, Jen AKY. Chemistry of Materials 2010;22(19):5601-5608.

[12] Shi ZW, Luo JD, Huang S, Polishak BM, Zhou XH, Liff S, Younkin TR, Block BA, Jen AKY. Journal of Materials Chemistry 2012;22(3):951-959.

[13] Zhou XH, Luo JD, Huang S, Kim TD, Shi ZW, Cheng YJ, Jang SH, Knorr DB, Overney RM, Jen AKY. Advanced Materials 2009;21(19):1976-1981.

[14] Gray T, Kim TD, Knorr DB, Luo JD, Jen AKY, Overney RM. Nano Letters 2008;8(2):754-759.

[15] Kim TD, Kang JW, Luo JD, Jang SH, Ka JW, Tucker N, Benedict JB, Dalton LR, Gray T, Overney RM, Park DH, Herman WN, Jen AKY. Journal of the American Chemical Society 2007;129(3):488-489.

[16] Luo JD, Ma H, Haller M, Jen AKY, Barto RR. Chemical Communications 2002(8):888-889.

[17] Ma H, Jen AKY. Advanced Materials 2001;13(15):1201-+.

[18] Luo JD, Haller M, Ma H, Liu S, Kim TD, Tian YQ, Chen BQ, Jang SH, Dalton LR, Jen AKY. Journal of Physical Chemistry B 2004;108(25):8523-8530.

[19] Luo JD, Liu S, Haller M, Liu L, Ma H, Jen AKY. Advanced Materials 2002;14(23):1763-+.

[20] Kolli B, Mishra SP, Joshi MP, Mohan SR, Dhami TS, Samui AB. Journal of Polymer Science Part a-Polymer Chemistry 2012;50(8):1572-1578.

[21] Kim MS, Song MY, Jeon B, Lee JY. Polymer International 2012;61(12):1739-1744.

[22] Haller M, Luo JD, Li HX, Kim TD, Liao Y, Robinson BH, Dalton LR, Jen AKY. Macromolecules 2004;37(3):688-690.

[23] Kang JW, Kim TD, Luo J, Haller M, Jen AKY. Applied Physics Letters 2005;87(7).

[24] Kim TD, Luo JD, Ka JW, Hau S, Tian YQ, Shi ZW, Tucker NM, Jang SH, Kang JW, Jen AKY. Advanced Materials 2006;18(22):3038-+.

[25] Kim TD, Luo JD, Tian YQ, Ka JW, Tucker NM, Haller M, Kang JW, Jen AKY. Macromolecules 2006;39(5):1676-1680.

[26] Luo JD, Haller M, Li HX, Kim TD, Jen AKY. Advanced Materials 2003;15(19):1635-+.

[27] Braunecker WA, Matyjaszewski K. Progress in Polymer Science 2007;32(1):93-146.
[28] Jenkins AD, Jones RG, Moad G. Pure and Applied Chemistry 2010;82(2):483-491.
[29] Georges MK, Veregin RPN, Kazmaier PM, Hamer GK. Macromolecules 1993;26(11):2987-2988.
[30] Nicolas J, Guillaneuf Y, Lefay C, Bertin D, Gigmes D, Charleux B. Progress in Polymer Science 2013;38(1):63-235.
[31] Kato M, Kamigaito M, Sawamoto M, Higashimura T. Macromolecules 1995;28(5):1721-1723.
[32] Wang JS, Matyjaszewski K. Journal of the American Chemical Society 1995;117(20):5614-5615.
[33] Chiefari J, Chong YK, Ercole F, Krstina J, Jeffery J, Le TPT, Mayadunne RTA, Meijs GF, Moad CL, Moad G, Rizzardo E, Thang SH. Macromolecules 1998;31(16):5559-5562.
[34] Moad G, Rizzardo E, Thang SH. Australian Journal of Chemistry 2012;65(8):985-1076.
[35] Debuigne A, Poli R, Jerome C, Jerome R, Detrembleur C. Progress in Polymer Science 2009;34(3):211-239.
[36] Yamago S, Iida K, Yoshida J. Journal of the American Chemical Society 2002;124(12):2874-2875.
[37] Higaki Y, Otsuka H, Endo T, Takahara A. Macromolecules 2003;36(5):1494-1499.
[38] Higaki Y, Otsuka H, Takahara A. Polymer 2003;44(23):7095-7101.
[39] Higaki Y, Otsuka H, Takahara A. Polymer 2006;47(11):3784-3791.
[40] Motokucho S, Sudo A, Sanda F, Endo T. Chemical Communications 2002(17):1946-1947.
[41] You YZ, Hong CY, Pan CY. Chemical Communications 2002(23):2800-2801.
[42] You YZ, Hong CY, Wang WP, Wang PH, Lu WQ, Pan CY. Macromolecules 2004;37(19):7140-7145.
[43] Hong J, Wang Q, Fan ZQ. Macromolecular Rapid Communications 2006;27(1):57-62.
[44] Jia Z, Liu C, Huang J. Polymer 2006;47(22):7615-7620.
[45] Zhang LS, Wang Q, Lei P, Wang X, Wang CY, Cai L. Journal of Polymer Science Part a-Polymer Chemistry 2007;45(13):2617-2623.
[46] Liu YQ, Cavicchi KA. Macromolecular Chemistry and Physics 2009;210(19):1647-1653.
[47] Wu YS, Wang Q. Journal of Polymer Science Part a-Polymer Chemistry 2010;48(11):2425-2429.
[48] Ebeling B, Vana P. Macromolecules 2013;46(27):4862−4871.
[49] Ebeling B, Vana P. Polymers 2011;3(2):719-739.
[50] Zhang C, Wang Q. Journal of Polymer Science Part a-Polymer Chemistry 2011;49(3):612-618.
[51] Zhu QQ, Wang Q. Journal of Polymer Science Part a-Polymer Chemistry 2012;50(10):2029-2036.
[52] Nicolay R, Marx L, Hemery P, Matyjaszewski K. Macromolecules 2007;40(26):9217-9223.
[53] Greene AC, Zhu JH, Pochan DJ, Jia XQ, Kiick KL. Macromolecules 2011;44(7):1942-1951.
[54] Luo K, Yang JY, Kopeckova P, Kopecek J. Macromolecules 2011;44(8):2481-2488.
[55] Ebeling B, Eggers M, Vana P. Macromolecules 2010;43(24):10283-10290.
[56] Mita I, Stepto RFT, Suter UW. Pure and Applied Chemistry 1994;66(12):2483-2486.

[57] Senyek. 2002.
[58] Brandrup J, Immergut EH, Grulke EA. Polymer Handbook, 4th edition ed.: Wiley-Interscience, 1999.
[59] Moad G, Solomon DH. The Chemistry of Free Radical Polymerization, 2nd ed.: Elsevier: Amsterdam, 2006.
[60] Escalé P, Ting SRS, Khoukh A, Rubatat L, Save M, Stenzel MH, Billon L. Macromolecules 2011;44(15):5911-5919.
[61] Matyjaszewski K, Davis TP. Handbook of radical polymerization Ed.; Wiley-Interscience: Hoboken, 2002.
[62] Pawlik G, Rau I, Kajzar F, Mitus AC. Optics Express 2010;18(18):18793-18804.

Electronic Supplementary Information

Well-Defined Second-Order Nonlinear Optical Polymers by Controlled Radical Polymerization, via Multifunctional Macromolecular Chain Transfer Agent: Design, Synthesis, and Characterizations.

Anne-Lise Roy, [a] Chong Bui, [a] Ileana Rau, [d] François Kajzar, [d,e] Bernadette Charleux, [c] Maud Save, [b] David Kreher, [a,f] André-Jean Attias* [a]

[a] UMR 7610 CNRS – UPMC, Laboratoire de Chimie des Polymères, 3 rue Galilée, 94200 Ivry, France. E-mail: andre-jean.attias@upmc.fr.
[b] IPREM Equipe de Physique et Chimie des Polymères, UMR 5254 CNRS, Université de Pau et des Pays de L'Adour, Hélioparc, 2 Avenue du Président Angot, 64053 Pau Cedex, France.
[c] Chemistry, Catalysis, Polymers and Processes (UMR 5265), Université de Lyon, Bât. F308, B.P. 2077, 43 Bd du 11 Nov. 1918, 69616 Villeurbanne Cedex, France,
[d] University POLITEHNICA of Bucharest, Faculty of Applied Chemistry and Materials Science, Dept. of General Chemistry, 1 Polizu Street, 011061 Bucharest, Romania,
[e] Institut des Sciences et Technologies Moléculaires d'Angers, MOLTECH Anjou – UMR CNRS 6200, Angers University, 2 bd Lavoisier, 49045 Angers Cedex, France
[f] ENSTA – Synthèse Organique et Réactivité, Ecole Polytechnique – UMR CNRS 7652, 91128 Palaiseau Cedex, France

Experimental

Figure SI-1 shows the propagation length dependence of the scattered light from the planar waveguide made of studied films.

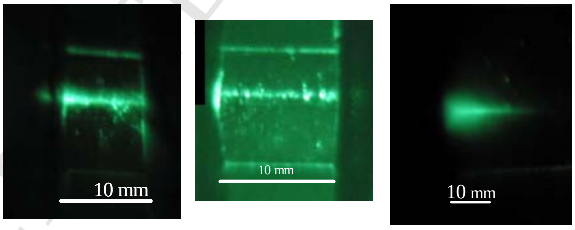

Figure SI-1. Propagation length dependence of scattered light from planar waveguide at 830 nm.

The derived optical propagation losses are listed in **Table SI-1**. The propagation losses increase with the chromophore concentration, as it is already observed **in Figure SI-1**, where the attenuation of the propagated light is the largest for the most concentrated film.

Chromophore concentration	2.3	5	7.1
Propagation losses (dB/cm)	6.8	10	12.7

Table SI-1: Propagation losses in studied films at 830 nm

We observe increase of propagation losses with concentration . Most likely it is due to two factors:

(i) residual absorption of chromophores (measurements are done at 830 nm, thus not very far from the absorption band) and absorption of harmonics of O-H and C-H vibrations
(ii) Light scattering by aggregates
(iii) Residual impurities

It is well known that strong dipole-dipole interaction of dipolar CT chromophores leads to their aggregation, thus to large propagation losses. However the aggregation effect strongly increases with the chromophore concentration. If it was the case of propagation losses we should observe much larger propagation losses at higher chromophore concentration. We observe a less than proportional increase, what is in favour of second point.
Impurities may contribute to the scattering losses too. Although our polymers were carefully purified, we cannot exclude their presence in. They may either absorb and/or scatter light..

Chromophores were oriented by the corona poling technique :[1]
To remember, usually in corona poling method, a high voltage (6-8 kV) applied to a needle electrode distant by 1.5 to 2.5 cm from the thin film surface creates the ionization of the surrounding atmosphere. The second bottom electrode is planar (usually ITO covered glass plate, on which is deposited the poled film). The substrate supporting the thin film is put on a heating block and the film is heated close to the glass transition temperature to increase the orientational mobility of poled chromophores. Depending on the sign of the potential applied to the needle electrode, positive or negative charges are created and cover the thin film surface, creating a large electric field between the thin film surface and the bottom electrode. Usually the poling time is short, a few minutes and the created polar order is afterwards frozen by cooling the film to room temperature. More details can be found in reference 3.
Concerning our setup, in order to increase the chromophore rotational mobility, the films were heated to the glass transition temperature. Than a high voltage of 6-8 kV was applied to the needle electrode, distant by about 15 mm from the poled film (**Figure SI-2**). The corona discharge ionizes the air around the electrode and depending on the sign of the applied electric field to the needle electrode those of the same sign are repelled and deposited on the film surface creating a large (~ 2-3 MV/cm) electric field inside. As said before, the bottom electrode usually is a thin layer of ITO, but the conductivity of BK7 glass used here is sufficient, so the glass substrate itself acts as electrode. The metallic grid, located between the film and the needle electrode (**Figure SI-2**) serves to control the poling current (for details see reference 2).

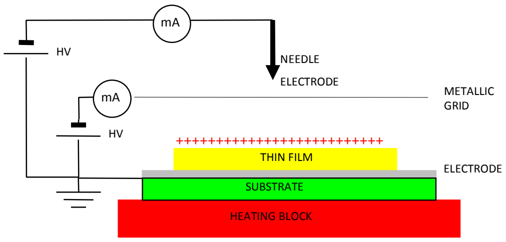

Figure SI-2. Schematic representation of the corona poling set up (note 3)

The optical absorption spectra of thin films were collected using a UV-VIS Perkins Elmer spectrophotometer, model lambda 16. The thin film propagation losses were determined by imaging the scattered light from the planar waveguide. Its refractive indices were measured by m-lines technique using standard Metricon prism coupler system.

The SHG measurements were performed using a set-up described in reference 4 (cf. also Rau and Kajzar [5]). The light source is a Q switched Neodymium doped Yttrium Aluminium Garnet (Nd:YAG) laser, operating at 1 064.2 nm fundamental wavelength with pulse duration of 13 nanoseconds and 10 Hz repetition rate. The sample was mounted on a goniometer and rotated along an axis perpendicular to the beam propagation direction, coinciding with it. The SHG intensities were collected as function of the incidence angle. The input polarization was set by using a half wave plate, whereas the generated harmonic field polarization by a polarizer in fixed position, selecting p harmonic beam. In order to get the two nonzero tensor components for poled films with point symmetry ∞mm: $\chi^{(2)}_{XXZ} = 2d_{sp}$ and $\chi^{(2)}_{ZZZ} = 2d_{pp}$, the measurements were done in s-p and p-p fundamental – harmonic beam polarization. Here Z is the direction perpendicular to the film and X is within in the laboratory reference frame, respectively. For the f and h fundamental –harmonic beam polarization configuration the SHG intensity is given (cf reference 4 as well as the work of Swalen and Kajzar.[6])

$$I^{ffh}_{2\omega}(\theta) = \frac{32\pi^3}{c^2}\left|\frac{\chi^{(2)}_{ffh}(-2\omega;\omega,\omega)}{\Delta\varepsilon}-\right|^2 \left|T_{fh}(\theta)A_{fh}(\theta)\right|^2 \left| e^{i\Delta\varphi_{ffh}} -1 \right|^2 I^2_{\omega} \qquad (1)$$

where T_{fh} (θ) and A_{fh} (θ) are, respectively, incidence angle dependent factors arising from transmission and boundary conditions, I_ω is the incident light intensity and $\Delta\varphi$ is the phase mismatch between the fundamental and harmonic beam in the studied film, given by

$$\Delta\varphi_{ffh} = \varphi^f_\omega - \varphi^h_{2\omega} = \frac{4\pi\ l}{\lambda_\omega}\left(n^f_\omega \cos\theta^f_\omega - n_{2\omega}\cos\theta^h_{2\omega}\right) \qquad (2)$$

where ω(2ω) refers to the fundamental (harmonic) frequency, respectively. $\theta^{f(h)}_{\omega(2\omega)}$ are propagation angles in nonlinear medium for f(h) polarization of the beam with frequency ω(2ω), respectively.

The effective $\chi^{(2)}_{IJK}$ susceptibilities in Eq. (1), for a given fundamental –harmonic beam polarization configurations contain the projection factors and are given by

$$\chi^{(2)}_{ssp}(-2\omega;\omega,\omega) = 2d_{sp}\sin 2\theta^s_\omega \cos\theta^s_{2\omega} \qquad (3)$$

for s-p fundamental harmonic beam polarization, and

$$\chi^{(2)}_{ppp}(-2\omega;\omega,\omega) = 2d_{pp}\sin^2\theta^p_\omega \sin\theta^p_{2\omega} + 2d^{(}_{sp}\cos\theta^p_\omega(\cos\theta^p_\omega + 2\sin\theta^p_\omega \cos\theta^p_{2\omega}) \qquad (4)$$

where we took account of the usually used notations for the second order NLO susceptibility tensor components: $\chi^{(2)}_{XXZ}(-2\omega;\omega,\omega) = 2d_{sp}(-2\omega;\omega,\omega)$ and $\chi^{(2)}_{ZZZ}(-2\omega;\omega,\omega) = 2d_{pp}(-2\omega;\omega,\omega)$. Equations (3) - (4) show that the determination of both tensor components requires two independent measurements in s-p and p-p fundamental – harmonic beams polarization configurations. First measurements gives the off diagonal value $\chi_{sp}^{(2)}$. The second (p-p) configuration measurements will yield the diagonal $\chi_{pp}^{(2)}$ susceptibility, injecting the previously determined value of $\chi_{sp}^{(2)}$ into Eq. (4).

The SHG intensities were calibrated with SHG measurements performed on an y-cut slab of α-quartz. For the calibration we used the value reported by Choy and Byer (d_{11} = 0.5 pm/V).[7]

As detailed in the article, for weight concentrations of DR19 lower than 7 %, the second harmonic generation (SHG) coefficients (d_{sp} and d_{pp}) increase linearly with the chromophore concentration (see **Figure SI-3**). Moreover, even taking into account of the experimental uncertainty (± 10 %) we observe a chromophore concentration dependence of both d_{sp} and d_{pp} coefficients. This observation is in favor of the absence (or limited) of aggregation in synthesized functional polymers.

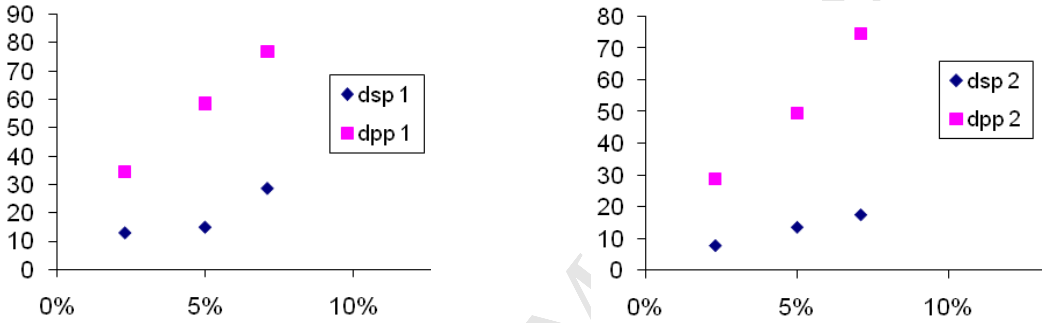

Figure SI-3. Second -order NLO susceptibilities d_{sp} and d_{pp} of the thin polymer films containing the DR19 chromophore at different weight concentrations fractions. The precision in d coefficient determination is ±10%. Evolution of (dsp and dpp) NLO coefficients of polymers as a function of the DR19 loading density.

Calculation procedure of d_{pp} value for reference 8 of the article (Banach, M. J.; Alexander, M. D.; Caracci, S.; Vaia, R. A. *Chemistry of Materials* **1999**, *11*, 2554-2561):

In this precedent study, very small electro-optic coefficient r_{33} of 0.4 pm/V was measured by the modulated ellipsometry technique at 780 nm wavelength, in thin film of polystyrene containing 10 wt% concentration of disperse red 1 (DR1) chromophore. The relationship between the electro-optic (EO) $\chi^{(2)}(-\omega;\omega,0)$ susceptibility and the electro-optic coefficient r_{pp} (Burland, D.; Miller, R.; Walsh, C. *Chem. Rev*. **1994**, *94*, 31) is as follows:

$$\chi_{pp}^{(2)}(-\omega;\omega,0)=\frac{n^{4'}}{2}r_{pp}(-\omega;\omega,0)$$

where n is the index of refraction at ω frequency and taking n = 1.62 (cf. Fig 2 of the article) one gets $\chi_{pp}^{(2)}(-\omega;\omega,0)$ = 1.7 pm/V. Assuming that both susceptibilities EO and SHG are close ($\chi_{pp}^{(2)}(-2\omega;\omega,\omega)\approx\chi_{pp}^{(2)}(-\omega;\omega,0)$), d_{pp} was calculated to be 0.85 pm.V^{-1}.

---

[1] Comizzoli, B. *J. Electrochem. Soc.: Solid Science and Technology* **1987**, *134*: 424.
[2] Kajzar, F.; Lee, K.-S.; Jen, A; K.-Y. *Advances in Polymer Science* **2002**, *161*, 1.
[3] from F. Kajzar and J.-M. Nunzi, Molecule Orientation Techniques, in Beam Shaping and Control with Nonlinear Optics, F. Kajzar and R. Reinisch, Eds, NATO ASI Series, Series B : Physics, vol. 369, Plenum Press, New York 1998, pp. 101-132)
[4] Rau, I.; Armatys, P.; Chollet, P.-A.; Kajzar, F.; Andraud, C.; Bretonnière, Y. Linear and nonlinear optical properties of a new guest host system, Nonl. Opt. Quant. Opt., **35**, 57-67, (2007).
[5] I. Rau and F. Kajzar, Second harmonic generation an its applications, Nonl. Opt. Quant. Opt.,38, 99-140(2008)
[6] J. Swalen and F. Kajzar. Introduction, in Organic Thin Films for Waveguiding Nonlinear Optics, F. Kajzar and J. Swalen Eds, Gordon & Breach Sc. Publ., Amsterdam 1996, pp. 1-44
[7] Choy, M.; Byer, R. L. *Phys. Rev. B.* **1976**, *14*, 1693.